Scanning Microscopy

Volume 6 | Number 2 Article 22

4-21-1992

Particle Induced X-Ray Emission Microanalysis of Root Samples from Beech (Fagus sylvatica)

M. Hult
Lund Institute of Technology

B. Bengtsson
Swedish University of Agriculture

N. P. -O. Larsson
Lund Institute of Technology

C. Yang
Shanghai Institute of Nuclear Research

Scanning Microscopy, Vol. 6, No. 2, 1992 (Pages 581-590) 0891-7035/92$5.00+.00
Scanning Microscopy International, Chicago (AMF O'Hare), IL 60666 USA

PARTICLE INDUCED X-RAY EMISSION MICROANALYSIS OF ROOT SAMPLES FROM BEECH (*FAGUS SYLVATICA*)

M.Hult[1,*], B.Bengtsson[2], N.P.-O.Larsson[1], C.Yang[3]

1)Lund Institute of Technology, Dept. of Nuclear Physics, Lund, Sweden
2)Swedish University of Agriculture, Dept. of Horticulture, Alnarp, Sweden
3)Shanghai Institute of Nuclear Research, Shanghai, China. Presently at: Lund Institute of Technology

(Received for publication November 25, 1991, and in revised form April 21, 1992)

Abstract

Beech seedlings (*Fagus Sylvatica*) were grown in a nutrient solution to which $AlCl_3$ had been added. The experiments were designed to evaluate the effect of aluminum on the localization of elements in plant root tissue. Cross-sections of roots were analyzed with micro-PIXE (particle induced X-ray emission) and Rutherford backscattering (RBS) simultaneously. A proton beam of either 30x30 μm^2 or 5x5 μm^2 was scanned over the samples, and quantitative elemental maps were created. Aluminum was found to accumulate in high concentrations (percent levels) in the epidermis and the outer layer of the cortex, when the nutrient solution held 1.0 mM $AlCl_3$. It was also obvious that calcium was depleted where aluminum accumulated. The distribution of aluminum was inhomogeneous, and therefore, it was necessary to analyze the total area of the cross-section and not only look at a small part of it, for example along a diametrical line.

Key Words: Acidification, aluminum, beech, calcium, elemental mapping, microprobe, quantitative, particle induced X-ray emission (PIXE), roots, Rutherford backscattering spectrometry (RBS).

*Address for correspondence:
Mikael Hult
Lund Institute of Technology
Department of Nuclear Physics
Sölvegatan 14
S-223 62 Lund
Sweden.

Phone no.:+46 46 107741
Fax no.:+46 46 104709

Introduction

A decrease in forest growth has been reported since around 1950, and large scale forest dieback in central Europe and Eastern USA became a reality during the 70s and 80s (Shortle and Smith, 1988). There is no doubt that this phenomenon is related to the increased emission of acidifying gases and other air pollutants (Ulrich, 1985). The vitality of the trees is most certainly affected both by direct exposure to air pollutants and by changes in soil chemistry due to acidification. A pH decrease in soil solution is accompanied by a loss of base cations (Ca^{2+}, Mg^{2+} and K^+) and an increase in Al^{3+} (Tyler, 1987). When the pH drops below 4.5, the Al^{3+} concentration in the soil solution increases drastically (Bergkvist, 1987). The forest decline is most certainly a multiple stress phenomenon, but the detrimental effects of aluminum on plants indicate that it may be one of the major stress factors if present in crucial amounts (Asp, 1991).

One purpose of this investigation is to describe and quantify the localization of aluminum in beech roots and also to determine if aluminum affects the distribution of other elements in the root. To accomplish this task, root samples were analyzed with a nuclear microprobe (NM) using particle induced X-ray emission (PIXE) and Rutherford backscattering spectrometry (RBS) simultaneously. PIXE has proved to be an excellent technique to detect trace elements in biological samples (Maenhaut, 1990), (Malmqvist, 1986), (Johansson and Campbell, 1988), and the micro-PIXE technique is especially interesting when studying biological samples with large cell structures (Vis, 1985a). Plant root tissue has been studied by e.g. Makjanic et al. (1988) and hamster tooth germs have been studied with micro-PIXE by Lyaruu et al. (1990). Other methods, like radioactive tracers, have been used to determine the uptake of different minerals in beech plants (Bengtsson et al., 1988), but the distribution of trace and minor elements inside the root has not been completely determined.

Another purpose of this investigation is to show that it is possible to create quantitative maps of elements with the micro-PIXE technique and to optimize the conditions for analyzing trace and minor elements in root tissue at micrometer resolution level.

Materials and Methods

Germination and Cultivation

Seeds of beech (*Fagus Sylvatica L. provenance Scania*) from Sweden were germinated according to Bengtsson et al. (1988). The seedlings were mounted in plastic foam holders and grown in blackpainted 2 liter beakers containing 1.5 l of nutrient solution of the following composition: 0.1 mM KH_2PO_4, 0.1 mM $Ca(NO_3)_2$, 0.2 mM KNO_3, 0.1 mM $MgSO_4$, 20 µM Fe-EDTA; 0.36 µM $MnSO_4$, 0.048 µM $CuCl_2$, 0.78 nM Na_2MoO_4, 0.42 nM $ZnSO_4$ and 0.37 µM H_3BO_3. After 2 weeks the seedlings were transferred to a climate chamber with a temperature of 20 ± 1^{o} C. Light was provided by 400 W Philips HQl lamps giving a light intensity of about 30 Wm^{-2}. From this point, the seedlings were grown in two different continuously aerated nutrient solutions. The first group of seedlings was a control, which received no $AlCl_3$ in the nutrient solution. The second group received nutrient solution to which 1.0 mM $AlCl_3$ had been added. The pH was kept at 4.2, and the nutrient solution was renewed twice a week during the treatment period of 18 days.

Specimen Preparation

A 20 mm piece of root from the main root tip was cut with a scalpel and immediately frozen in liquid nitrogen. The frozen root samples were stored in small bottles at -80^{o}C until the cryosectioning. The root was fixed by the use of an embedding medium (Tissue-Tek™ O.C.T. 4583 Compound) before the sectioning at -20^{o}C. The cross-sections were cut 10 mm from the tip, and the object thickness was 20 µm. The sections were then put on a plastic foil (Kimfol™), which was mounted on a circular holder. The holder was carefully lifted up from the microtome some 20 centimeters for a couple of seconds so that a temporary increase of temperature occurred. This made the embedding medium adhesive to the plastic foil. Finally the samples were freeze-dried and stored in a desiccator until elemental analysis. To avoid movement of elements in the samples during preparation, the temperature was maintained below -5^{o}C in the fresh samples before freezedrying.

The PIXE- and RBS-Setup

The freeze-dried roots were placed in a new versatile specimen chamber (Themner et al., 1991), where the PIXE- and RBS-analyses were performed. The samples were irradiated with 1.0 MeV protons from a 3 MV electrostatic tandem accelerator (NEC 3UDH) at normal incidence to the target. The specimen chamber and the accelerator are coupled to the Lund nuclear microprobe, the most important components of which are a slit system, a beam scanning system and a focussing system. This nuclear microprobe has been described in some recent papers (Malmqvist et al., 1989b), (Pallon et al., 1990), (Tapper et al., 1990).

The X-rays from the samples were detected with a Si(Li)-detector (Kevex™, area: 30 mm^2) placed at an angle of 135^{o} relative to the incident beam. The Si(Li)-detector had a Be-window of 8 µm and an external filter of 7 µm Mylar™. In order to determine the light matrix elements (carbon, nitrogen and oxygen), backscattered protons were detected at 165^{o} relative to the incident beam with a surface barrier detector (Ortec™, area: 25 mm^2).

In this work,the proton beam has been focussed either to $(30 \pm 4) \times (30 \pm 4)$ μm^2 or $(5 \pm 1) \times (5 \pm 1)$ μm^2 and when scanning has been performed, each step has been either (30 ± 0.3) or (5 0.05) µm. The beam size was determined by looking in a microscope at the fluorescence from a quartz plate when it was hit by the microbeam. The relative uncertainty in beam size can be estimated to be 10% and 20% for the large and small beam size respectively. The current has typically been 1 nA for the large beam spot and 0.1 nA for the small beam spot. The beam was moved over the target with a preset time for irradiation of each pixel of 200 ms. Data was collected until the number of pulses was considered enough for an accurate quantification (e.g. 2.7 hours in fig.2.)

The data acquisition and beam scanning control system consists of a micro-VAX-II host computer and a front-end computer system based on a VME-bus (Malmqvist et al., 1989a), (Lövestam, 1989). During this scanning NM analysis, data was collected event-by-event and stored on a 0.5 GByte Winchester disk.

Quantitative Evaluation

Because many elements play important roles in the living cell, it is advantageous to study as many of them as possible at the same time with a method like PIXE. But while the PIXE-method can analyze several elements simultaneously the sensitivity is different for different elements. In this work, the analysis parameters were adjusted so that X-ray detection was optimized for the elements Mg, Al, Si, P, S, Cl, K and Ca. These elements were also determined quantitatively.

Protons with an energy of 2.55 MeV are routinely used for PIXE analysis in Lund and yield a high sensitivity for elements in the range Z=25-35. The sensitivity is, however, relatively poor for light elements in the range Z=11-13 (Na, Mg and Al) since a filter, for example 75 µm beryllium, is required to stop scattered protons from interacting with the detector crystal. By lowering the proton energy, we can reduce the filter thickness. However, that reduction comes at the expense of a decrease in the cross-sections for X-ray production. At a proton energy of 1 MeV, the K production cross-section for Na (Z=11) is 25% lower compared to 2.55 MeV protons and for Zn it is a factor of 10 lower. On the other hand the transmission of K_α X-rays from Na (1.041 keV) through 7 µm Mylar™ and 8 µm beryllium (which are required to stop 1 MeV protons) is a factor of 50 higher than the 2.55 MeV case, where 75 µm beryllium has to be used as a filter (3.7% vs. 0.075%). A PIXE-spectrum from a beech root sample analyzed with 1 MeV protons is presented in figure 1.

The PIXE-setup was calibrated using a previously reported procedure (Johansson et al., 1981) with thin standards from Micromatter™. The RBS-

calibration was performed on plastic foils (Kapton™ and Kimfol™). In order to calculate the concentrations of the elements detected in the PIXE analysis, the matrix elements carbon, nitrogen and oxygen were measured using RBS with 1 MeV protons.

A scanning NM analysis creates an extensive data set. (For example a scan of 64x64 pixels will create 4096 PIXE and RBS spectra.) If the data is collected event-by-event, as in this work, time information will be generated. The drawback of event-by-event collection is that the datafiles will continue to grow as long as data is collected.

Once the event-by-event data was sorted into pixel spectra, the RBS spectra were evaluated to determine the carbon, nitrogen and oxygen amounts. An automatic algorithm (Hult and Themner, 1990), HCNO_MAP, implemented in FORTRAN-77 on the micro-VAX-II computer was used to evaluate the one thousand RBS spectra at a speed of 0.3-0.4 s/spectrum. The original computer code was optimized to handle data from biological samples that were analyzed with 2.55 MeV protons. A new version was implemented, which could handle data from an analysis with 1.0 MeV protons. It was not beneficial for the RBS analysis to lower the proton energy to 1.0 MeV because the carbon, nitrogen and oxygen signals were overlapping more than in the 2.55 MeV case. Also the maximum thickness of the sample had to be lowered from 2.0 mg/cm^2 to 0.8 mg/cm^2 since, if the samples were thicker, the protons scattered in the bottom layer would have too little energy to reach the detector. The thickness of the root samples varied from 0.1 mg/cm^2 to 0.6 mg/cm^2 and was typically 0.4 mg/cm^2. The output from HCNO_MAP is the sample thickness in μg/cm^2 (assuming that the matrix elements are hydrogen, carbon, nitrogen and oxygen). Hydrogen cannot be detected using RBS. Instead a well-established value for the hydrogen content was used. It has been found that the hydrogen content in freeze-dried plant tissue is fairly constant around 6% (Salisbury and Ross, 1985), and therefore, this figure was used in all calculations.

The PIXE-spectra were evaluated with the GEOPIXE code (fig.1)(Ryan et al. 1988,1990). Each spectrum took approximately 30 seconds to evaluate, which resulted in reasonable evaluation times for our maps that never were larger than 25x25 pixels (5 hours). After the evaluation of each pixel-spectrum, which resulted in elemental concentrations in dry weight, the elemental maps were assembled.

Mass Loss.

The NM does undoubtedly cause radiation damage and mass loss in the irradiated tissue

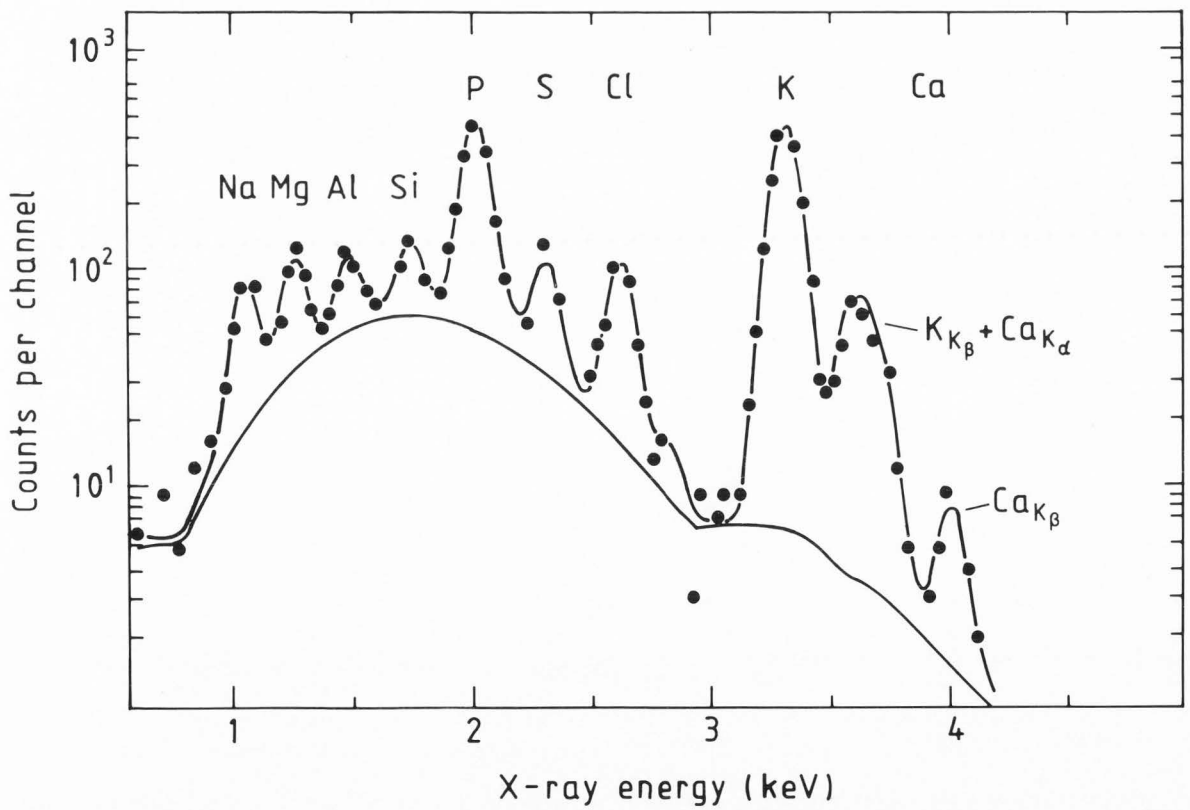

Figure 1. PIXE spectrum from a root sample that has been irradiated with 1 MeV protons. The data points have been fitted using the computer code GEOPIXE. The solid lines show the background fit and the total fit.

(Themner et al., 1990). During the analysis, the count rate was monitored both for the PIXE and RBS signal but no decrease could be noted. Since data was collected event-by-event, it was possible to sort the data into several spectra from the same spot taken at different times. No mass loss could be proved for any of the elements detected in the PIXE analysis. A slight but not significant decrease from 243 counts·nC^{-1} to 230 counts·nC^{-1} could be noticed in the count rate for the elements carbon,nitrogen and oxygen in the RBS spectra corresponding to the sample in figure 2. This sample was irradiated with a 30x30 μm^2 beam and the accumulated charge in each spot was approximately 14.4 nC, which would correspond to a dose of 4x10^9 Gy. Themner et al. (1990) noticed that the mass loss was serious for oxygen and hydrogen. According to their measurements,there would be an expected loss of 20% hydrogen and 50% oxygen. The evaluation of RBS-spectra from different time intervals indicates that the oxygen loss was less than 50% (approximately 20%). Most of the oxygen is, however, supposed to be lost within the first microseconds, and this loss could not be detected since each pixel was irradiated 200 ms at a time. Therefore, our mass data was corrected for 50% oxygen loss.

Results

The first sign of how aluminum affected the plant was discovered during the sample preparation. The samples which had been cultivated with $AlCl_3$ in the nutrient solution were more brittle than the others. PIXE analysis of the control group revealed that the samples were clean. That is to say that not one single spot with Al above detection limit could be found. The detection limit for Al was dependent on the accumulated charge in each spot and varied from 50 μg/g to 400 μg/g, but was typically 150 μg/g in the spots analyzed in this investigation. Table 1 shows the detection limits, in a typical pixel, for all elements that were detected in the PIXE analysis. The distribution of sodium was also determined but not quantified.

Table 1. Detection limits in ppm (μg/g) and fg/pixel (dry weight) for the elements that were determined in the PIXE analysis. The values are taken from a pixel, which has been irradiated with a 30x30 μm^2 beam and an accumulated charge of 10 nC. The areal mass density was 0.4 mg/cm^2.

Element	Detection Limit (ppm)	(fg/pixel)
Mg	250	900
Al	150	540
Si	120	430
P	95	340
S	80	290
Cl	75	270
K	70	250
Ca	60	220

One sample from each of the groups (control and 1.0 mM $AlCl_3$) was analyzed with a 30x30 μm^2 beam. The results were presented as elemental maps like the figures 2a-2c. Line scans, with a 5x5 μm^2 beam (fig.3a-3c, 4a and 4b), were also made in order to increase the lateral resolution. Since the maximum number of pixels to be scanned in the x- and y-direction is 64, three scans had to be made to analyze the diametrical line indicated in the schematic drawing in figure 3a. The different scans are indicated with the Roman numbers I-III for the $AlCl_3$ treated sample (fig. 3a-3c) and with IV-V for the control sample (fig.4a-4b). The irradiation time for the scan in figure 2 was 162 minutes, while the irradiation time for the 5 line scans (I-V) in figure 3 and 4 were 282, 128, 90, 274 and 68 minutes respectively.

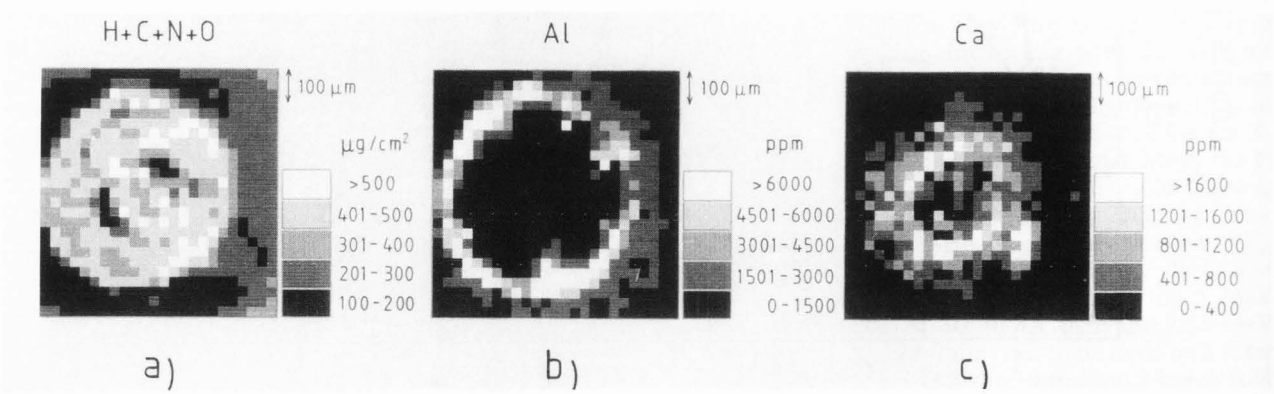

Figure 2. Elemental dry weight-concentrations and distributions from a root cultivated in a solution to which 1.0 mM $AlCl_3$ has been added. The maps are made up of 25x25 pixels; each pixel is 30x30 μm^2. a) The matrix elements H, C, N and O. (6% hydrogen has been assumed.) b) The Al concentration. c) The Ca concentration. The total irradiation time for the scan was 2.7 hours.

These results indicate that aluminum accumulated in high concentrations in the epidermis and the outer layers of the cortex, which can be seen in figure 2 and 3. Aluminum effectively depleted calcium in this region (figs. 2c, 3a and 4a). Extracellular calcium, bound to cell walls and plasma membranes, was most likely displaced by monomeric aluminum (Al^{3+}, $Al(OH)^{2+}$), since the binding capacity of monomeric aluminum is much higher than for Ca^{2+}.

Figure 2b and 3b show that in some spots the aluminum concentration reached percent levels, and that it was inhomogeneously distributed along the peripheral cortex as well as in the cortical and vascular tissue of the root cross section. The calcium concentration for the sample from the 1 mM-group was higher in the cortical tissue next to the endodermis and decreased to a couple of hundred μg/g in the stele (fig.3a). The phosphorus concentration was higher in the peripheral cortex than in the inner cortex (fig.3c) and the vascular concentration was higher than in the cortex. A comparison between the control sample (fig.4b) and the sample from the 1 mM-group (fig.3c) shows no significant differences in phosphorus concentration.

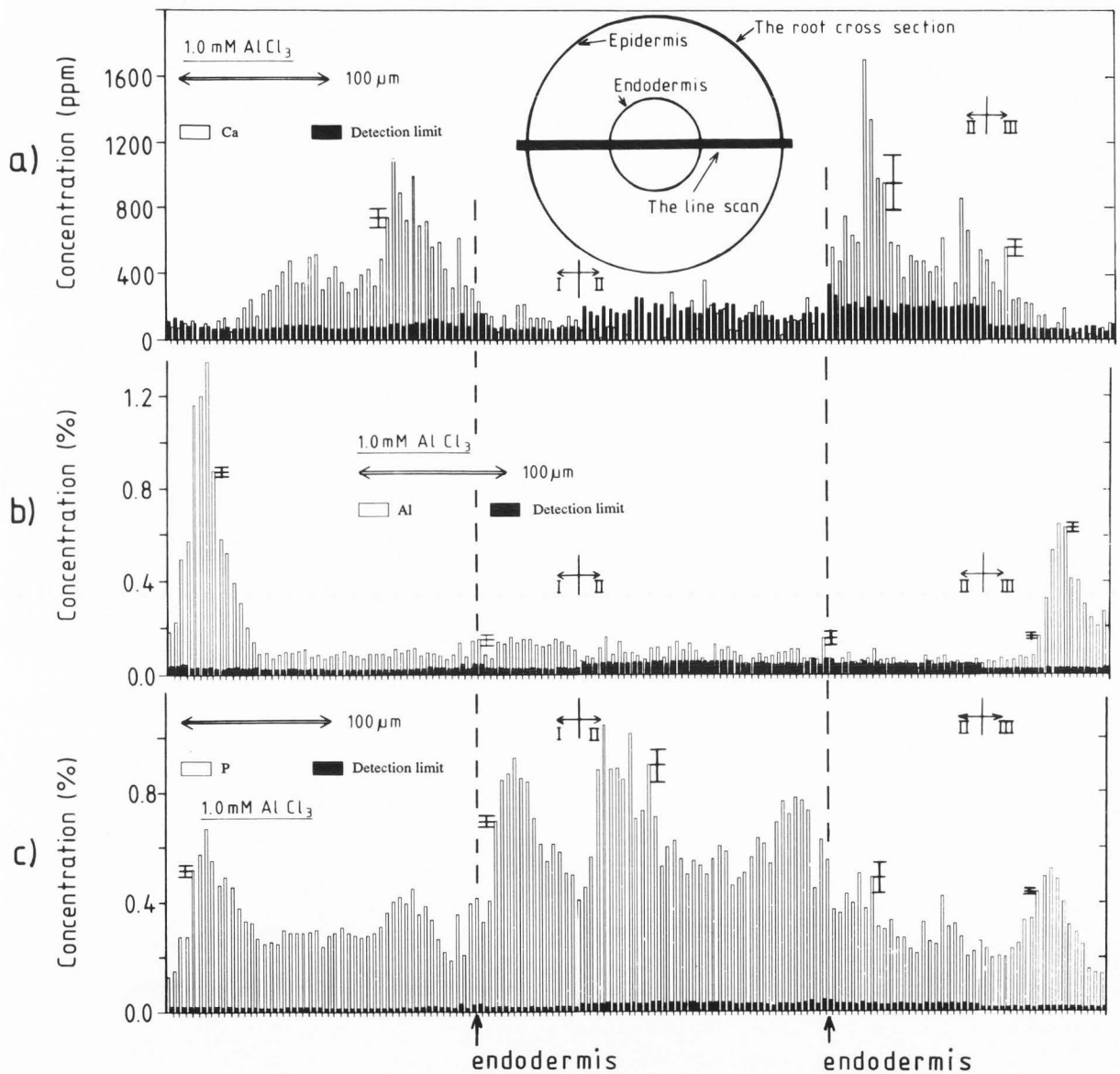

Figure 3. Elemental dry weight-concentrations and distributions from a root cultivated in a solution to which 1.0 mM $AlCl_3$ has been added. Each pixel is 5x5 μm^2. The line scan is indicated in the schematic drawing of the root and is 150 pixels long (64+64+22). The numbers I to III indicate the three different sections of the line scan. The error-bars indicate the statistical uncertainty at some pixels. a) Ca, b) Al, c) P.

One would expect aluminum phosphate to be formed in the area which coincided with high aluminum concentrations (McCormick and Borden, 1974), but this can not be seen.

In the figures 3a-3c, 4a and 4b, the statistical uncertainty has been indicated at some pixels. There are, however, a couple of other sources of uncertainty in the PIXE- and RBS- evaluation that have to be taken into account. Tabulated values of scattering cross sections, stopping cross sections and X-ray production cross sections have an uncertainty of approximately 10% each. Minor uncertainties (<5%) comes from X-ray attenuation in the sample, high Al-concentrations in the sample and the calibration procedure. Another problem is the mass loss of oxygen, which was discussed in the previous section.

To facilitate recognition of structures in the root sample, some elemental maps have been smoothed. This procedure gives the picture smoother borderlines, but will also give a false impression of increased spatial resolution. To avoid erroneous conclusions, the original picture has always been used together with the smoothed one. In the smoothing procedure, each pixel is divided into 3x3 pixels. A simple form of smoothing with general applicability is the bilinear interpolation (see e.g. Press et al., 1987). This interpolation has been used here. The value of each new pixel is a linear combination of the original pixel and the surrounding eight original pixels. The smoothing procedure can be performed twice and thus creating pictures with 81 times as many pixels as the original pictures. Figure 5 shows the potassium concentration in the 1 mM $AlCl_3$ case and in the control sample, where the original map has been smoothed and each original pixel has been divided into 9x9 new ones.

Discussion and Conclusions

The micro-PIXE technique is a powerful tool which might be of tremendous use for biologists as well as for other scientists. It is, however, necessary to develop the technique so that quantitative maps of elements at micrometer resolution level can be obtained more routinely. The major problems are the time-consuming analysis and evaluation. A new single-ended 3 MV electrostatic accelerator (NEC 3UH) has recently begun operation in Lund. Higher

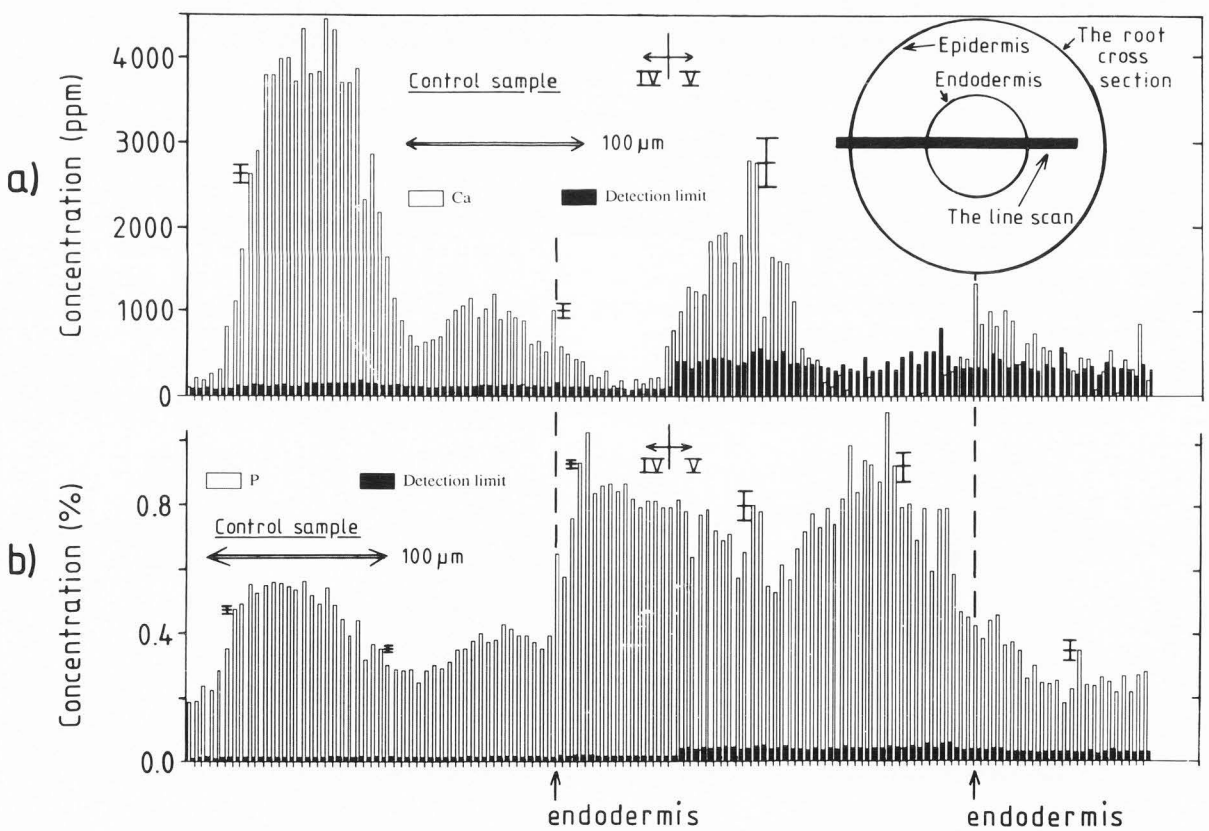

Figure 4. Elemental dry weight-concentrations and distributions from a root in the control group. No aluminum could be detected in any pixel. Each pixel is 5x5 μm^2. The line scan is indicated in the schematic drawing of the root and is 128 pixels long (64+64). The numbers IV to V indicate the two different sections of the line scan. The error-bars indicate the statistical uncertainty at some pixels. a) Ca, b) P.

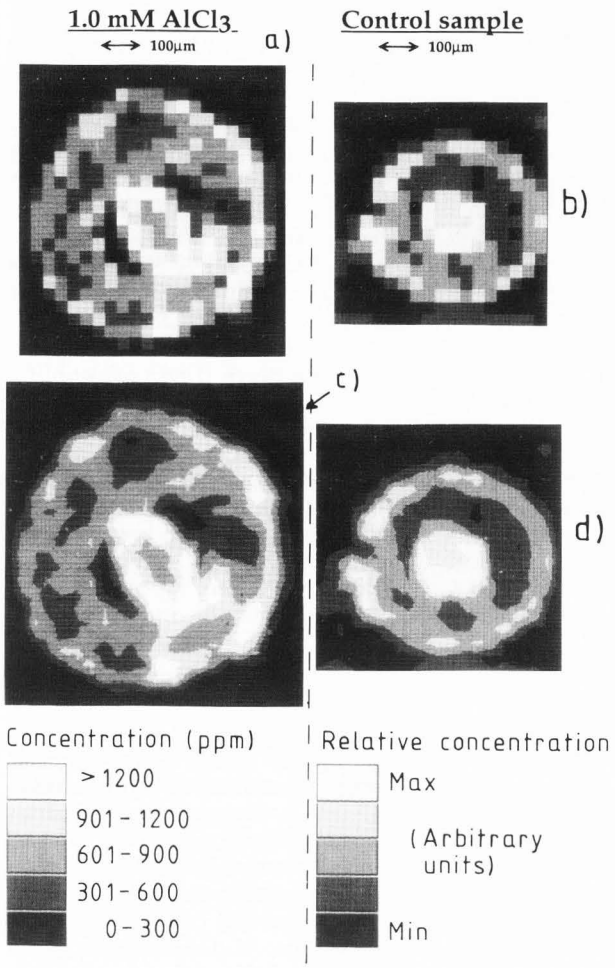

Figure 5. The potassium dry weight-concentration and distribution in maps consisting of original data: a) 1.0 mM $AlCl_3$ b) Control sample, and smoothed data: c) 1.0 mM $AlCl_3$ d) Control sample.

stability and brightness is expected from this machine, which will increase the current density and, thus, make analysis time shorter.

To minimize analysis time, it is important not to analyze pixels that are of no interest (e.g. pixels beside the sample). If an irregular scan (the area that is to be scanned can be of any shape, not only rectangular) is made, only the relevant pixels might be analyzed. In the case of a circular root sample, there would be a 20% reduction in the number of analyzed pixels compared to a rectangular scan.

When analyzing samples like those in this study, it is inappropriate to make scans along diametrical lines since many elements are more or less inhomogeneously distributed. This investigation shows that in this particular case it is preferable to analyze fewer samples and, instead, scan the whole area. We plan to analyze more samples and will try to use a beam size of 8x8 μm^2, which will make it possible to scan the complete root cross section if the root cross sections, like in this work, are 500 μm in diameter (64 pixels x 8 μm = 512 μm). Minimizing analysis time is very important considering that to achieve detection limits of 50 μg/g for Al with a 8x8 μm^2 beam and a beam current of 0.25 nA (which is possible today), the analysis time would be around 56 hours (16 s/pixel). With the new machine it will be possible to get at least 1 nA beam current within 8x8 μm^2

Having taken into account the uncertainty of the elemental concentrations and distributions, still a lot of biological conclusions can be drawn. The effective depletion of calcium by aluminum probably affects the calcium homeostasis outside the cytoplasm. Disturbance of the extracellular calcium balance is probably the primary event which initiates the symptoms of aluminum toxicity. The endodermal layer, which surrounds the vascular tissue is not detected as a barrier to aluminum radial transport since no concentration shift is obvious. This is contrary to what Jentscke et al. (1991) found for *picea* roots. The endodermis, however, acts as a barrier to calcium transport towards the stele. The extracellular transport of calcium is prevented by suberinization and forming of the Casparian strip.

Acknowledgements

We are grateful to the National Swedish Environmental Protection Agency (SNV) and The Royal Swedish Academy of Agriculture and Forestry for financial support.

References

Asp H (1991) Influence of Aluminium on Mineral Uptake by Beech *(Fagus sylvatica)* and Spruce *(Picea abies)* Roots. Academic Dissertation, Department of Plant Physiology, University of Lund, Sweden, 10-20.

Bengtsson B, Asp H, Jensén P, Berggren D (1988) Influence of Aluminium on Phosphate and Calcium Uptake in Beech *(Fagus sylvatica)* Grown in Nutrient Solution and Soil Solution. Physiol. Plant. 74:299-305.

Bergkvist B (1987) Leaching of Metal from Forest Soils as Influenced by Tree Species and Management. For. Ecol. Manage. 22:29-56.

Hult M, Themner K (1990) Quantitative Microanalysis of Matrix Elements in Biological Samples by MeV Proton Scattering. Nucl. Instr. and Meth. B50:154-158.

Jentschke G, Schlegel H and Godbold DL (1991) The Effect of Aluminium on Uptake and Distribution of Magnesium and Calcium in Roots of Mycorrhizal Norway Spruce Seedlings. Physiol. Plant. 82:266-270.

Johansson GI, Pallon J, Malmqvist KG, Akselsson KR (1981) Calibration and Long-Term Stability of a PIXE Set-up. Nucl. Instr. and Meth. 181:81-88.

Johansson SAE, Campbell JL (1988) PIXE - A Novel Technique for Elemental Analysis. J. Wiley & Sons, Chichester UK, 177-199.

Lyaruu DM, Tros GHJ, Bronckers ALJJ, Wöltgens JHM (1990) Micro-PIXE (Proton Induced X-ray Emission) Study of the Effect of Fluoride on Mineral Distribution Patterns in Enamel and Dentin in the Developing Hamster Tooth Germ. Scanning Microsc. 4, 315-322.

Lövestam G (1989) Development of the Lund Proton Microprobe Scanning and Data Acquisition System. Nucl. Instr. and Meth. B36:455-470.

Maenhaut W (1990) Multielement Analysis of Biological Materials by Particle-induced X-ray Emission (PIXE). Scanning Microsc. 4, 43-62.

Makjanic J, Vis RD, Groneman AF, Gommers FJ, Henstra S (1988) Investigation of P and S Distributions in the Roots of *Tagetes patula* L. Using Micro-PIXE. J. Experim. Botany 39, 208:1523-1528.

Malmqvist KG (1986) Proton Microprobe Analysis in Biology. Scanning Elect. Microsc. 1986;III:821-845.

Malmqvist KG, Lövestam NEG, Pallon J, Tapper UAS (1989a) Data Acquisition and Presentation in Scanning Nuclear Microprobe Analysis. Scanning Microsc. 3, 785-795.

Malmqvist KG, Asking L, Hansson H-C, Hellborg R, Hyltén G, Johansson E-M, Johansson SAE, Kristiansson P, Larsson P, Lövestam NEG, Martinsson BG, Pallon J, Svantesson B, Swietlicki E, Tapper UAS, Themner K (1989b) PIXE and Proton Microprobe Advances at the Lund Institute of Technology. Nucl. Instr. and Meth. B40/41:685-689.

McCormick LH, Borden YF (1974) The Occurrence of Aluminum-Phosphate Precipitate in Plant Roots. Soil Sci. Soc. Amer. Proc., 38, 931-934.

Pallon J, Johansson SAE, Hult M, Hyltén G, Kristiansson P, Larsson P, Lövestam NEG, Tapper UAS, Themner K (1990) Recent Advances in the Nuclear Microprobe at the Lund Institute of Technology. Nucl. Instr. and Meth. B45:548-552.

Press WH, Flannery BP, Teukolsky SA, Vetterling WT (1987) Numerical Recipes. The Art of Scientific Computing, Cambridge University Press, Cambridge, 95-101.

Ryan CG, Clayton E, Cousens DR, Griffin WL, Sie SH (1988) SNIP, A Statistics-sensitive Background Treatment for the Quantificative Analysis of PIXE Spectra in Geoscience Applications. Nucl. Instr. and Meth. B34:396-402.

Ryan CG, Cousens DR, Griffin WL, Sie SH, Suter GF (1990) Quantitative PIXE Microanalysis of Geological Material Using the CSIRO Proton Microprobe. Nucl. Instr. and Meth. B47:55-71.

Salisbury FB and Ross CW (1985) Plant Physiology, 3rd edition. 103-104.

Shortle WC, Smith KT (1988) Aluminium-Induced Calcium Deficiency Syndrome in Declining Red Spruce. Science 240:1017-1018.

Tapper UAS, Hellborg R, Hult M, Larsson NP-O, Lövestam NEG, Malmqvist KG, Pallon J, Tapper UAS, Themner K (1990) The Lund Nuclear Microprobe: Instrumentation, Data Collection and Data Evaluation. Nucl. Instr. and Meth. B49:425-429.

Themner K, Spanne P, Jones KW (1990) Mass Loss During X-ray Microanalysis. Nucl. Instr. and Meth. B49:52-59.

Themner K, Hult M, Hyltén G, Håkansson K, Larsson NP-O, Lövestam NEG, Nilsson L-B, Pallon J, Tapper UAS, Malmqvist KG (1991) A New Versatile Specimen Chamber for the Lund Scanning Nuclear Microprobe. Nucl. Instr. and Meth. B54:38-41.

Tyler G (1987) Acidificatioon and Chemical Properties of South Swedish Beech (*Fagus Sylvatica L.*) Forest Soil. Scand. J. For. Res. 2:263-271.

Ulrich B (1985) Interaction of Indirect and Direct Effects of Air Pollutants in Forests. In: Air Pollution and Plants, C. Troyanowski , (ed.), VCH Verlagsgesellschaft, Weinheim, 149-181.

Vis RD (1985a) The Proton Microprobe: Applications in the Biomedical Field. CRC Press Inc., Boca Raton, Florida, 146-155.

Discussion with Reviewers

D.L. Godbold: The authors could not show that the endodermis acts as a barrier to Al using the PIXE technique. Using X-ray microanalysis and making measurements on cell walls, an endodermis barrier has been shown by a number of authors for several species including beech. It has also been shown that at high levels of Al, Al accumulates not only in the cell walls but in the protoplast of the outer cortex cells, which would account for the Al distribution pattern found by the authors. Would the authors agree that they could not show a barrier to the radial transport of Al, as the technique used makes a blanket measurement of all cell structures and not the points of accumulation such as the cell walls?

Authors: If the endodermis acts as a barrier to aluminum you would expect increased levels of aluminum outside of the endodermal layer as could be seen for calcium. The apoplastic transport of aluminum is probably not as pronounced as for calcium. A symplastic radial transport of aluminum, not as Al^{3+} or other monomeric forms, but chelated could be the reason that we do not get a step in concentration in the region of the endodermal layer. Also, we have to be aware of the longitudinal transport along primarily developed vessel elements from apical regions of the root. This transport complicates the evaluation of data and the discussion of whether the endodermis acts as a barrier to radial transport.

We must agree that the lateral resolution of the PIXE analysis as used in this study does not allow focussing on cell compartments. However, sensitivity for trace elements is better than with an electron probe.

W. Maenhaut: Is there a particular reason why this study was performed on beech? Is the beech perhaps more susceptible to Al intoxication than other trees or is it one of the most common plants in Scandinavian forests? Also, why was the root of this plant studied and not some other part (e.g. stem, branches, leaves)?
Authors: Beech, compared to e.g. spruce and pine, normally grows on more alkaline soils and is less adapted to the release of monomeric Al. The primary toxic effect of aluminum on plant development is on the mineral uptake mechanism. That is why roots were analyzed, but it would of course be interesting to continue this research by analyzing other parts of the plant. Also, beech is common in the southern part of Sweden.

G.M. Roomans: How do the authors know that Ca is removed by Al from an extracellular location?
Authors: Most calcium in roots is located extracellularly. The cytoplasmic free calcium is especially low. To investigate the uptake kinetics, experiments by use of ^{45}Ca have been performed. They have shown that especially the initial uptake, which refers to uptake in the extracellular compartment, is reduced by aluminum (Bengtsson, 1992).

W. Maenhaut: In the discussion section, you relate your total Ca concentrations to the transport of this element. However, only a certain fraction of the total calcium will be mobile Ca^{2+}. Do you have any idea how large this mobile fraction is?
Authors: In roots most calcium is mobile. The free Ca^{2+} fraction in the cytoplasm is submicromolar. However, Ca^{2+} binds to organic acids as oxalate or malate in the vacuolar compartment of leaves. In younger root parts, as has been analyzed in this study, we suppose 70-90% of calcium to be mobile or exchangeable.

G.M. Roomans: In fig 4a, there is a relatively high Ca concentration in the right half of the stele (the third "peak" at the beginning of scan V). How does that fit in with the endodermis being a barrier to Ca?
Authors: The calcium peak in the middle of the stele in the control plant (fig. 4a) is an interesting feature, which is not found in the Al-treated plant root. Transport of calcium from the apical parts of the root, where the endodermal layer is not fully developed and suberinized (Caspary's strip), may take place.

W. Maenhaut: According to fig. 2a, your specimen exhibited mass thickness variations that were up to a factor of 5 when using a 30x30 μm^2 beam size. How large were these variations for the linear scans shown in Figs. 3 and 4?
Authors: The thickness variation in pixels inside the sample in figure 2a is less than a factor of 4 (145-545 $\mu g/cm^2$). This is not possible to see in the picture but we still think that elemental maps like fig.2 and 5 are interesting and can give much information. The thickness variations for the linear scans in figure 3 and 4 were, however, larger than a factor of 4 (125-560 $\mu g/cm^2$ and 111-537 $\mu g/cm^2$ respectively).

The samples that were analyzed were carefully examined both before and after irradiation to check for cracks or other type of damage. This could not be seen on any of the analyzed samples.

R.D. Vis: What is the estimated error in the concentration values resulting from the assumption that 50% of all oxygen was lost in the very beginning of the irradiation?
Authors: The oxygen concentration in the matrix is approximately 40%. A rough estimate of a 68% confidence interval of the oxygen loss is 30-70%. This means that the uncertainty in the thickness due to the oxygen loss is approximately 10%. If other sources of uncertainty (which are mentioned under the result-heading) are combined in quadrature, the overall uncertainty of the concentration will be less than 25%. This figure varies of course between different pixels and different elements.

R.D. Vis: Do you have any suggestion as to how data can be collected on oxygen loss during the first micro-seconds of irradiation?
Authors: This is a very difficult task. However, STIM (Scanning Transmission Ion Microscopy) before and after PIXE would indicate the total mass loss even in the first μs. STIM, is a powerful analytical method where the energy of the projectile that has penetrated the sample is measured (Lefevre et al., 1987). The more energy the particle has lost, the "thicker" the target is. Few particles are required (one can be considered enough) to determine the target thickness and thus the mass loss induced by very low doses can be studied. It is, however, not possible to identify which elements are lost.

The beam intensity may be an important parameter, so perhaps a pulsed ion beam could be used to study the effect of e.g. 1 nA.

R.D. Vis: Is the $^{27}Al(p,p'\gamma)^{27}Al$ nuclear reaction, which has a high cross section using protons of 2.55 MeV, not a good or even better alternative for these analyses? According to my estimates, lower detection limits than reported here should be attainable.
Authors: This is a very interesting alternative for aluminum-detection. There are also high gamma-yields from Na using 2.55 Mev protons (Asking et al., 1987). In this investigation we are, however, interested in examining many low-Z elements (e.g. Na, Mg, P, S, K and Ca) apart from Al to study the effect of Al on other elements. Thus there is also the possibility of using multidimensional statistics to look for relationships between elements in the tissue that are impossible to observe when only studying one or two elements.

2.55 MeV protons can be considered to lose between 25 and 100 keV when penetrating the samples in this investigation. The gamma yield varies with the

proton energy. Even though the excitation function is known and is linear at some interval (Vis, 1985b), it is difficult to find an energy, where the gamma yield from Al as well as Na is constant after a proton energy loss of 100 keV (Asking et al., 1987), (Boni et al., 1988). Experimental difficulties may also arise because of problems with gamma-background from aluminum parts in the system.

W. Maenhaut: In order to optimize the sensitivity of the PIXE analysis for the lighter elements (Z=11-13), an incident proton energy of 1 MeV was used instead of the "normal" 2.55 MeV proton energy. By doing so, the scattered protons could be stopped with a much thinner absorber in front of the Si(Li) detector. But why was a 7 μm Mylar absorber used in addition to the 8 μm Be window of the detector? Instead of the Mylar absorber, an additional 8 μm Be absorber could have been used, and this would have resulted in a 6 times larger transmission for the Na K_α X-rays. Alternatively, by resorting to Be instead of Mylar, a higher beam energy (e.g., 1.5 MeV) could have been used while still maintaining the same X-ray transmission as in the present case, and at the same time, the sensitivity for an element like Zn would have been 3 times better.

Authors: It is true that the X-ray yield for the low-Z elements of interest in this study would be higher with an absorber entirely made of Be. Shortly after these PIXE-analyses were performed, the chamber was dismantled to be moved to a new accelerator specially dedicated for microanalysis with a NM and at the time of the measurements we did not have the opportunity to prepare the setup with another Be- absorber.

It is of interest to use alpha-particles of 4 MeV instead of protons (Johansson, 1992). The detection limit for Al would probably be lower because of the increased production cross section. The Be-window required to stop particles from entering the detector needs to be 18 μm. In the RBS spectra, peaks from different matrix elements are better resolved using α-particles.

Additional References

Asking L, Swietlicki E, Garg ML (1987) PIGE Analysis of Sodium in Thin Aerosol Samples. Nucl. Instr. and Meth. B22, 368-371.

Bengtsson BT (1992) Influence of Aluminium and Nitrogen on Uptake and Distribution of Minerals in Beech Roots (*Fagus Sylvatica*). Vegetatio, in press.

Boni C, Cereda E, Braga Marcazzan GM, de Tomasi V (1988) Prompt Gamma Emission Excitation Functions for PIGE Analysis of Li, B, F, Mg, Al and P in Thin Samples. Nucl. Instr. and Meth. B35, 80-86.

Johansson SAE (1992) Optimization of the Sensitivity in PIXE Analysis. International Journal of PIXE, 2, 33-46.

Lefevre HW, Schofield RMS, Overley JC, MacDonald JD (1987) Scanning Transmission Ion Microscopy as it Complements Particle Induced X-ray Emission. Scanning Microsc. 1, 879-889.

Vis RD (1985b) The Proton Microprobe: Applications in the Biomedical Field. CRC Press Inc., Boca Raton, Florida, 35-39.